Drift of sparse and dense spiral waves under joint external forces

Teng-Chao Li,[1,*] Qi-Hao Li,[2,*] Zhen Song,[2] De-Bei Pan,[3] Wei Zhong,[4,5] and Jinming Luo[6,†]

[1]*School of Physics, Hangzhou Normal University, Hangzhou 311121, China*

[2]*Peng Cheng Laboratory, Shenzhen, Guangdong 518066, China*

[3]*Department of Physics, Guangxi Medical University, Nanning 530021, China*

[4]*Guangdong Provincial Key Laboratory of Quantum Engineering and Quantum Materials and School of Physics and Telecommunication Engineering, South China Normal University, Guangzhou 510006, China*

[5]*Guangdong-Hong Kong Joint Laboratory of Quantum Matter, Frontier Research Institute for Physics, South China Normal University, Guangzhou 510006, China*

[6]*School of Mathematics, China University of Mining and Technology, Xuzhou 221008, China*

(Received 11 November 2022; accepted 7 February 2023; published 22 February 2023)

Many methods have been employed to investigate the drift behaviors of spiral waves in an effort to understand and control their dynamics. Drift behaviors of sparse and dense spirals induced by external forces have been investigated, yet they remain incompletely understood. Here we employ joint external forces to study and control the drift dynamics. First, sparse and dense spiral waves are synchronized by the suitable external current. Then, under another weak current or heterogeneity, the synchronized spirals undergo a directional drift, and the dependence of their drift velocity on the strength and frequency of the joint external force is studied.

DOI: 10.1103/PhysRevE.107.024213

I. INTRODUCTION

Spiral waves, clinically also called reentry, rotor, or driver, are spatiotemporal self-organizing structures formed in a broad range of excitable systems, such as the classical Belousov-Zhabotinsky (BZ) reaction [1], CO oxidation on platinum [2], retina of the eyes [3], and aggregations of *Dictyostelium discoideum* amoebae [4], and even cardiac tissues [5], where spiral drift is thought to be a possible underlying mechanism for life-threatening polymorphic ventricular tachycardia [6–8].

Clinically, high-voltage electric shock is one of the most effective therapies to terminate fibrillation by resetting electric activities in cardiac tissues. However, high-voltage electric shock will cause severe side effects such as myocardial damage [9–12]. To avoid the problems of previous traditional therapy, less-damage technology has been proposed, such as eliminating spiral waves by controlling their dynamics. Drift dynamics of excitable spiral waves have been extensively studied, especially under the influence of different external forces, including periodic force [13], illumination [14,15], heterogeneity [16,17], electric field [18,19], and magnetic field [20].

Interestingly, Krinsky *et al.* found that the sparse and dense spirals may drift in opposite directions induced by the same advective field [21]. Then Xu *et al.* and Sridhar *et al.* investigated the drift behaviors of sparse and dense spirals in heterogeneous media successively [16,17], and observed that the sparse spirals might drift anomalously, i.e., drifting toward the region with longer spiral rotation period. However, especially in cardiac tissues, how to control drift behaviors of sparse and dense spirals remains largely unexplored.

It has been known that spiral waves may be induced to drift resonantly by external periodic force, that is, the spiral adjusts its rotational frequency to an integer multiple of the external forcing frequency, and executes a net drift along a straight line. This directional drift of spiral waves subjected to the external periodic force has been confirmed experimentally and numerically [22–35]. Agladze *et al.* observed the resonant drift of spiral waves induced by illumination in a light-sensitive BZ reaction [13]. Recently, resonant drift of rigidly rotating and even meandering spirals were studied numerically by applying both a circularly polarized electric field and a periodic force [36].

In this paper, we investigate the drift behaviors of synchronized sparse and dense spiral waves under the influence of the external weak current and heterogeneity. The spiral wave is synchronized by the external current, which is induced by an ideal array of electrodes applying periodic anisotropic current stimulation in cardiac tissue. The array of electrodes has been proposed as the alternative low-energy technology to control electrical turbulence [37]. The electrode current we apply in this work is coupled with the intercellular current [38]. We find that drift behaviors of sparse spirals are more susceptible to the changes of the external current, and even can convert into normal drift from anomalous one. However, dense spiral drift dynamics are insensitive to external current changes.

II. MODEL AND METHODS

In the presence of external current, the two-variable Barkley model becomes [39]

$$\frac{\partial u}{\partial t} = \nabla^2 u + \frac{u(1-u)}{\varepsilon}\left(u - \frac{v+b}{a}\right) + I_{ex}, \tag{1a}$$

*These authors contributed equally to this work.

†Corresponding author: jemy_lau@cumt.edu.cn

$$\frac{\partial v}{\partial t} = u - v, \tag{1b}$$

where $u(x, y, t)$ and $v(x, y, t)$ are the transmembrane voltage (activator) and gate variable (inhibitor), respectively. Parameters a and b govern the local kinetics, and ε denotes the relative time scale between the voltage and gate variable. We use two sets of system parameters: one is $a = 0.55$, $b = 0.05$, and $\varepsilon = 0.02$ for the sparse spiral wave, the other is $a = 1.0$, $b = 0.03$, and $\varepsilon = 0.02$ for the dense one. The last term in Eq. (1a) can be specified by the function

$$\begin{aligned} I_{ex}(x, y, t) = -g\Big[& I_0 \cos \omega_e t [u(x+1, y, t) - u(x-1, y, t)] \\ & + I_0 \cos\left(\omega_e t + \frac{3\pi}{2}\right)[u(x, y+1, t) \\ & - u(x, y-1, t)]\Big], \end{aligned} \tag{2}$$

where I_0 and ω_e are the strength and angular frequency of the external current, respectively. We choose a constant intercellular conductance $g = 5$. The $u(x+1, y, t) - u(x-1, y, t)$ represents the intercellular voltage difference between neighboring cells in the x direction, while $u(x, y+1, t) - u(x, y-1, t)$ stands for the intercellular voltage difference in the y direction [38]. The external current is spatially anisotropic, and its strength changes with local intercellular current and time, so it can synchronize the spiral wave. We define the recorded activation frequency deviated by less than 0.1% from ω_e as a synchronized state, which is similar as described in [40].

Furthermore, we add the external weak current I_w whose strength is I_1 into Eq. (1a), which is also coupled with the intercellular current:

$$\frac{\partial u}{\partial t} = \nabla^2 u + \frac{u(1-u)}{\varepsilon}\left(u - \frac{v+b}{a}\right) + I_{ex} + I_w, \tag{3a}$$

$$\frac{\partial v}{\partial t} = u - v, \tag{3b}$$

$$I_w(x, y, t) = -g\{I_1[u(x+1, y, t) - u(x-1, y, t)]\}, \tag{3c}$$

or with moderate heterogeneities modeled by changing the parameter ε linearly in the parallel direction:

$$\frac{\partial u}{\partial t} = \nabla^2 u + \frac{u(1-u)}{\varepsilon}\left(u - \frac{v+b}{a}\right) + I_{ex}, \tag{4a}$$

$$\frac{\partial v}{\partial t} = u - v, \tag{4b}$$

$$\varepsilon = \varepsilon_0[1 + \delta(x - x_0)]. \tag{4c}$$

It should be noted that Eq. (3c) has a similar function as described in [18,41], i.e., a small constant field $\vec{e}$ of strength I_1 applied along the positive x axis. In this work, the joint external forces are composed of external current I_{ex} and weak current I_w (or heterogeneities ε). Equations (3) and (4) are integrated by an explicit Euler method with grids of size 500 × 500, and no-flux boundary conditions are used. The space and time steps are $\Delta x = \Delta y = 0.1$ and $\Delta t = 0.002\,375$, respectively. The midpoint position of the x component of the coordinates $x_0 = 25.05$ is used.

TABLE I. Frequency ranges of synchronized sparse spirals.

I_0	0.05	0.10	0.15	0.20	0.25
P	[1.0, 1.08]	[0.95, 1.09]	[0.91, 1.10]	[0.85, 1.12]	[0.8, 1.13]
I_0	0.30	0.35	0.40	0.45	0.50
P	[0.74, 1.15]	[0.67, 1.17]	[0.6, 1.18]	[0.53, 1.20]	[0.46, 1.22]

III. RESULTS

Figures 1(a) and 1(b) show the sparse and dense spirals with no external current, i.e., $I_{ex} = I_w = 0$, respectively. The excitation wavelength of the sparse spiral is $\lambda_{es} = c\tau = 1.4$ (c is the velocity of wave propagation and τ is the characteristic duration of the excitation waves for $u > 0.5$), which is much less than its spiral pitch $\lambda_s = 18.1$ ($\lambda_{es}/\lambda_s \ll 1$). Otherwise, the excitation wavelength of the dense spiral is $\lambda_{ed} = 3.6$, which is comparable to its pitch $\lambda_d = 9.9$ [$\lambda_{ed}/\lambda_d \sim \mathrm{O}(1)$] [21]. The rotation centers (or tips) of these spirals both execute rigid rotation, and the rotation period is $T_0 = 5.389$ for the sparse spiral, and $T_0 = 3.362$ for the dense.

Drift behaviors of these spirals induced by weak current and heterogeneity are studied in detail below. First, we apply the weak current to these spiral waves, and they are induced to drift in the opposite directions, as shown in Figs. 1(c) and 1(d). Next, we apply external current I_{ex} to synchronize the sparse and dense spirals. It means that the spiral is induced to accommodate its rotating frequency to the frequency of external current. In Tables I and II, as the strength of external current increases from 0 to 0.5, we show the ranges of the frequency ratio P ($P = \frac{\omega_e}{\omega_0}$, and $\omega_0 = \frac{2\pi}{T_0}$), with which the external current can synchronize the sparse and dense spirals, respectively. Obviously the sparse spiral is much easier to be synchronized compared with the dense one. Taking $I_0 = 0.4$, for example, the effective value of the ratio P is $P \in [0.6, 1.18]$ for the sparse spiral, while it is still very close to 1 for the dense one.

After that, another weak current is applied to the synchronized sparse and dense spirals. In Fig. 2, we show drift trajectories of synchronized spirals as the parameters of external current (I_0 and P) are changed. Obviously, the drift behaviors of sparse spirals are easier to be affected by the external current. Most notably, the synchronized sparse spiral may turn its drift direction to the right region under the influence of a weak current [in Figs. 2(a) and 2(c)]. Nevertheless, the drift direction of the synchronized dense spiral only exhibits a small change, as shown in Figs. 2(b) and 2(d).

Moreover, it is known that scroll waves exhibiting negative filament tension in a three-dimensional medium may develop into a turbulent state, and the filament tension coefficient is directly related to the spiral drift direction parallel to the weak current in a two-dimensional medium [41]. In this work, if the drift direction of the spiral wave is consistent with the positive direction of the x axis, the filament tension is positive, and if the drift direction of the spiral wave is opposite to the positive direction of the x axis, the filament tension is negative. Specifically, here the tension coefficient τ_e is taken as $\tau_e = \frac{v_x}{I_1}$, where v_x is the horizontal drift speed since the weak current is along the parallel direction. For the sparse spiral, as shown in Fig. 3, the filament tension coefficient keeps negative at $I_0 = 0.3$ no matter what values of the frequency

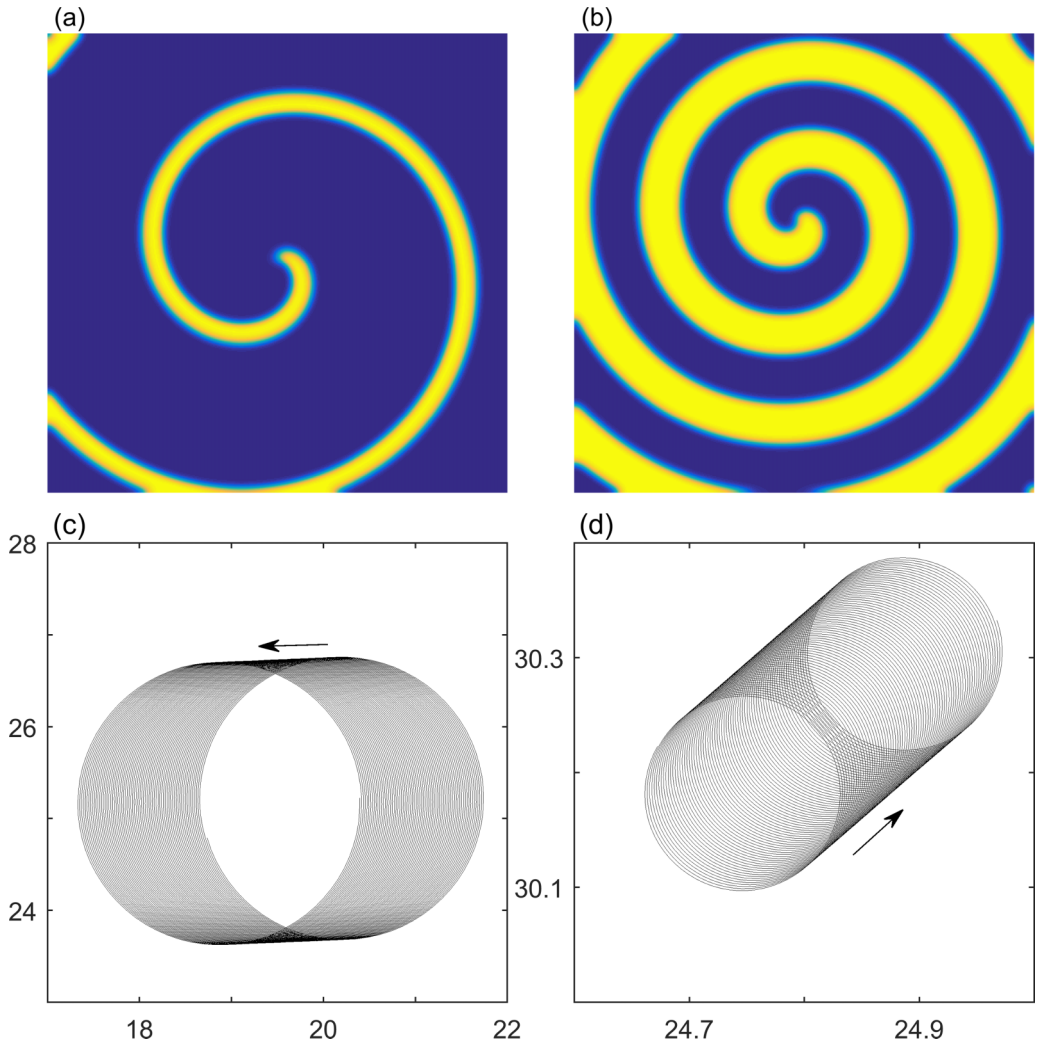

FIG. 1. Snapshots of a sparse spiral wave (a) and a dense spiral wave (b) without external current ($I_{ex} = I_w = 0$). Panels (c) and (d) are the drift trajectories of sparse and dense spirals induced by the external forces with parameters $\varepsilon = \varepsilon_0$, $I_0 = 0$, and $I_1 = 0.001$. The arrows denote the drift directions.

rate P [Figs. 3(a1) and 3(b1)]. As I_0 is increased over 0.3, τ_e turns positive if P is over a threshold value. But for the dense spiral, the filament tension coefficient is always positive, and the drift angle changes trivially with different parameters of external current (Fig. 4). Negative filament tension is one of the typical results causing cardiac arrhythmias [42,43]. Under the influence of the external current, the system can turn from the negative filament tension to the positive one, thus it is a possible low-energy method for cardiac defibrillation.

In the following, we study drift behaviors of sparse and dense spirals in the heterogeneous media, i.e., $\varepsilon = \varepsilon_0[1 + \delta(x - x_0)]$, where x denotes the spatial position along the parallel direction of the inhomogeneous gradient, and $x_0 = 25.05$ is the parallel midpoint position of the simulation domain. Fig. 5 shows drift trajectories of the spiral waves which are induced only by the heterogeneity. The sparse spiral drifts toward the left region of the higher excitability since a smaller ε enhances wave propagation, which means anomalous drift [Fig. 5(a)]. For comparison, the dense spiral drifts normally to the right region of the lower excitability [Fig. 5(b)] [17]. Then we apply external current to synchronize the sparse and dense spirals, and after that we study drift behaviors of

TABLE II. Frequency ranges of synchronized dense spirals.

I_0	0.05	0.10	0.15	0.20	0.25
P	[0.998, 1.001]	[0.996, 1.001]	[0.993, 1.002]	[0.989, 1.003]	[0.985, 1.004]
I_0	0.30	0.35	0.40	0.45	0.50
P	[0.98, 1.005]	[0.975, 1.005]	[0.97, 1.005]	[0.965, 1.005]	[0.959, 1.005]

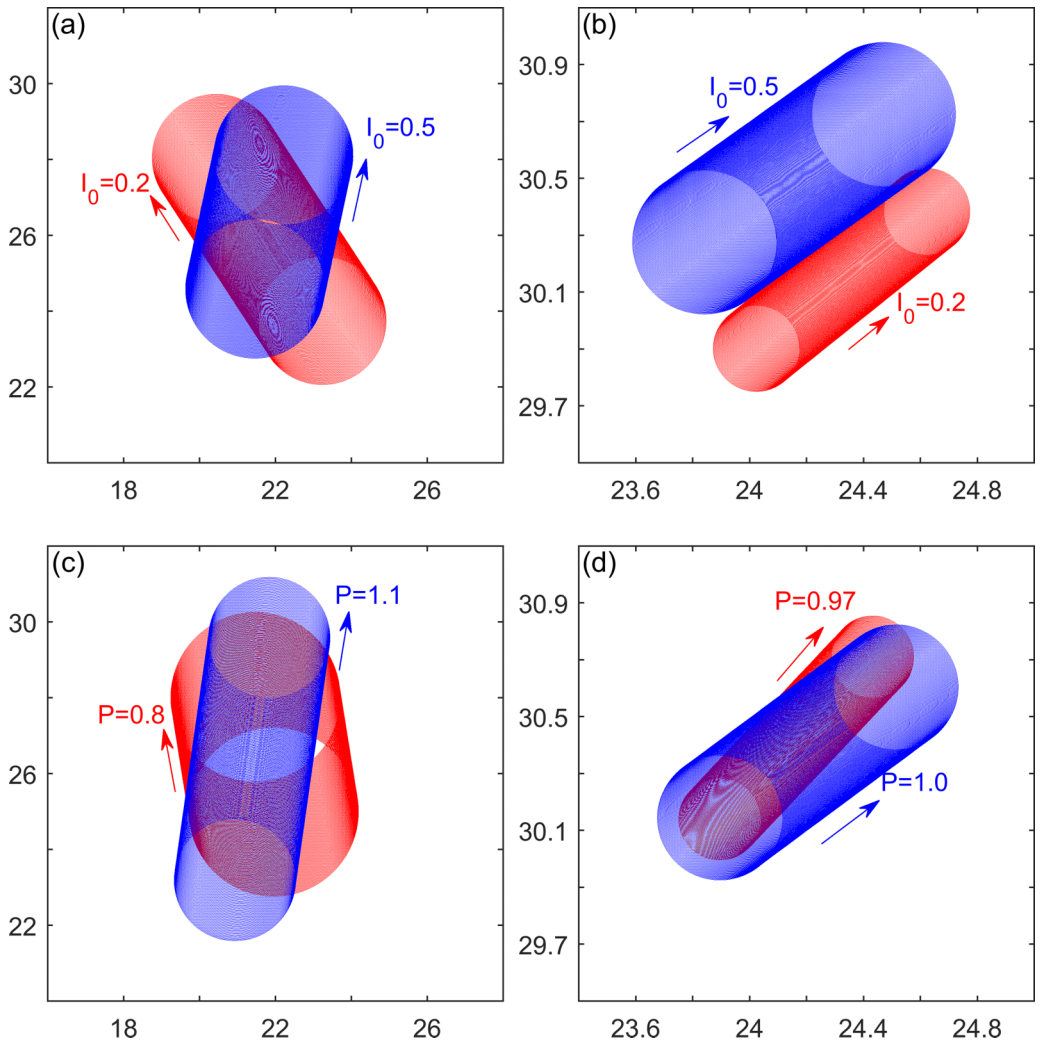

FIG. 2. Drift trajectories of synchronized sparse and dense spirals induced by the weak current with fixed strength $I_1 = 0.001$. Left column is for the sparse spirals and the right is for the dense ones. The parameters of external current are changed: (a) and (b) changing I_0 but fixing $P = 1$, (c) and (d) changing P but fixing $I_0 = 0.4$.

synchronized spirals in the heterogeneous media. As shown in Fig. 6, when I_0 is increased from 0 but fixing $P = 1$, the synchronized sparse spirals turn the anomalous drift to the normal drift quickly in the same heterogeneous medium [Fig. 6(a)]. Moreover, the drift direction of the sparse spiral is also sensitive to the frequency of external current [Fig. 6(c)]. On the contrary, drift behaviors of synchronized dense spirals induced by heterogeneities are still affected not much by the external current, as shown in Figs. 6(b) and 6(d).

Varying the parameters ε_0 and δ but keeping the external current I_{ex} fixed, we study the effects of heterogeneities on the drift behaviors of synchronized spirals. By increasing δ but fixing ε_0, as illustrated in Fig. 7(a), the drift speed of the sparse spiral increases, while the drift direction is almost unchanged. At increasing ε_0 but fixing δ, the changes of drift speed and direction of the dense spiral are both less sensitive, as shown in Fig. 7(b).

For comparison, without applying the external current, we calculate numerically drift speeds and angles of the sparse and dense spirals in the heterogeneous media by changing δ and ε_0. As shown in Figs. 8(a1) and 8(b1), the drift speeds of both sparse and dense spirals increase linearly with δ, which are similar to the observation in Fig. 7(a). Their drift angles increase slightly. Changing ε_0 but fixing δ, we observed that the drift speeds of sparse spirals change nonmonotonically with ε_0 [Fig. 8(c1)], and the drift angles decrease with ε_0 [Fig. 8(c2)]. On the other hand, the drift speeds and angles of dense spirals increase with ε_0 [Figs. 8(d1) and 8(d2)].

Finally, in Fig. 9, we show the drift speeds and angles of the synchronized sparse and dense spirals by varying the parameters (P and I_0) of the external current but fixing the heterogeneity parameters. Figure 9(a) shows the parabolic relations between the drift speed V of the sparse spirals and the frequency rate P of the external current. In Fig. 9(c), obviously the drift angle of the sparse spirals decreases as I_0 is increased, and is still anomalous for large P and $I_0 \leqslant 0.2$. In contrast, despite the relationships between the drift speeds (angles) of the dense spirals and $I_0(P)$ seeming complicated, the curves fluctuate within a narrow range, as shown in Figs. 9(b) and 9(d).

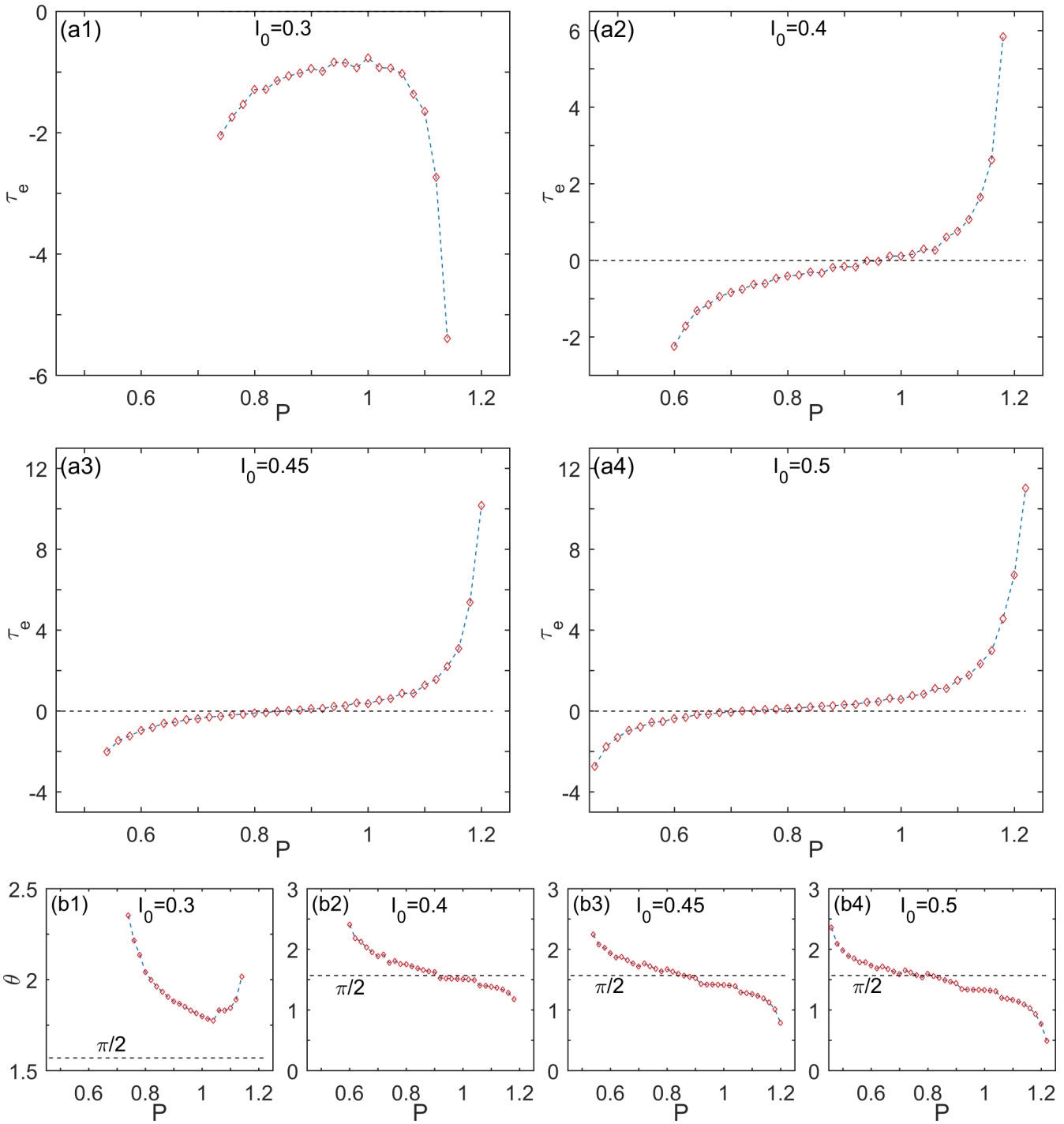

FIG. 3. Drift speeds and angles of the synchronized sparse spirals induced by the weak current with fixed strength $I_1 = 0.001$. The sparse spirals are synchronized by the external current with different strengths and frequencies.

IV. THEORY

The weak current or the heterogeneity can induce periodical changes in the core size and a directional drift of the rotating sparse and dense spirals, which results in drifts of these spirals. In the case of no external current, applying response function theory [18], we calculate theoretical drift speeds and angles of the sparse and dense spirals induced by the weak current, and they are quantitatively consistent with the numerical results. Taking the spiral waves in Fig. 1, for example, the theoretical values of their drift speed and angle are $V = |\dot{R}| = 4.193 \times 10^{-3}$ and $\theta = -3.059$ for the sparse one, and $V = |\dot{R}| = 7.895 \times 10^{-4}$ and $\theta = 0.729$ for the dense one, respectively. The numerical values of their drift speed and angle are $V = |\dot{R}| = 4.198 \times 10^{-3}$ and $\theta = -3.045$ for the sparse one, and $V = |\dot{R}| = 7.909 \times 10^{-4}$ and $\theta = 0.716$ for the dense one, respectively. Furthermore, according to the

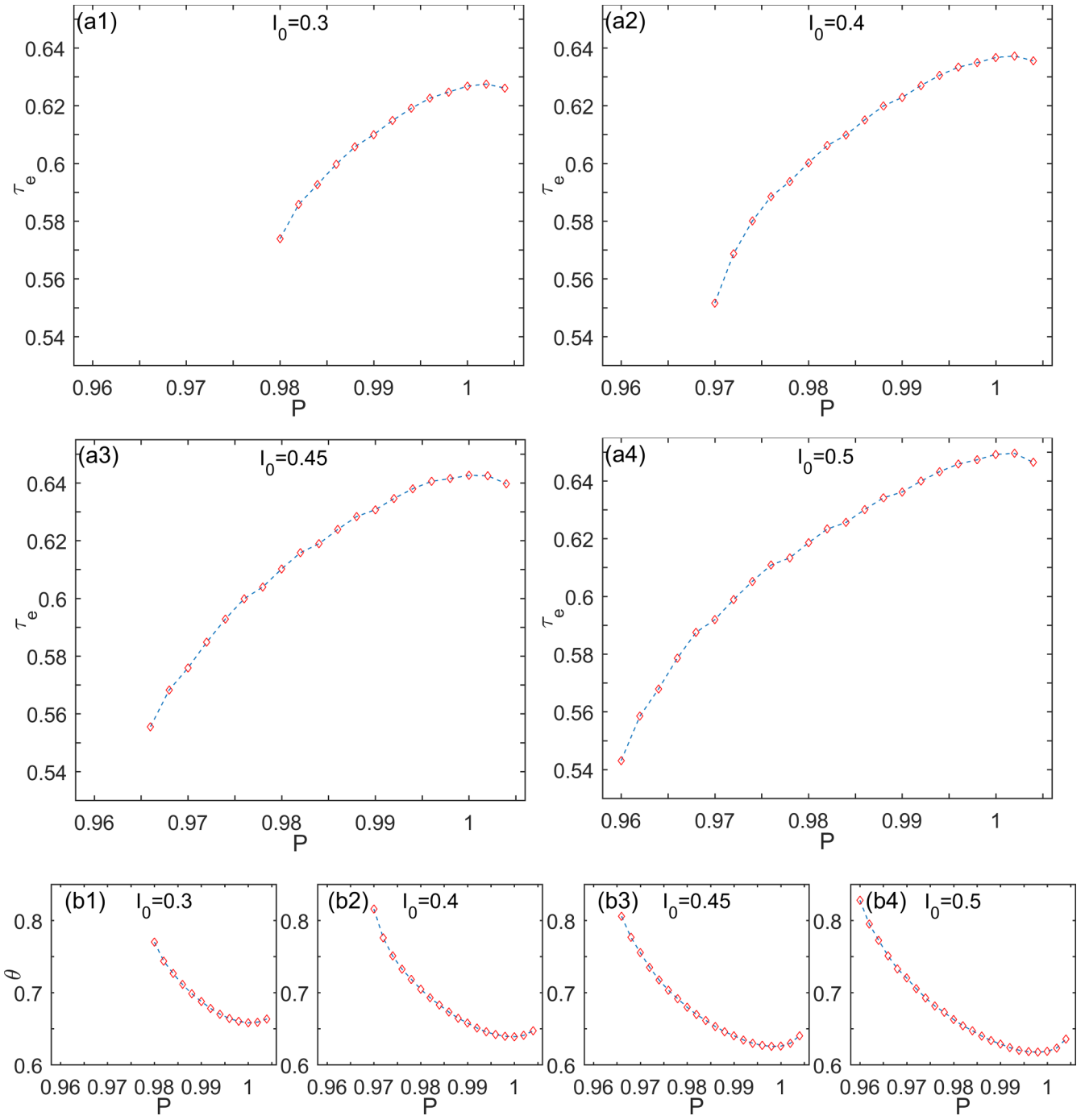

FIG. 4. Drift speeds and angles of the synchronized dense spirals induced by the weak current with fixed strength $I_1 = 0.001$. The dense spirals are synchronized by the external current with different strengths and frequencies.

derivation in [41,44,45], one obtains

$$\tau_e = \frac{V}{I_1}\cos\theta, \tag{5}$$

which shows that the sign of the filament tension coefficient is directly dependent on the drift direction. As shown in Fig. 3, τ_e is negative if the drift angle $\theta > \frac{\pi}{2}$, i.e., the sparse spiral drifts antiparallel to the weak current.

We also deduce theoretical drift speeds and angles of the sparse and dense spirals in heterogeneous excitable media without external current, and the results are as follows (more details can be found in the Appendix):

$$\dot{R} = \varepsilon_0\delta\Big\langle W^{(1)}(\rho,\theta,\Phi),\ \Big[-\frac{1}{\varepsilon^2}U(1-U)\Big(U-\frac{V+b}{a}\Big)\Big] \times \rho\frac{e^{-i\theta}}{2}|_{\Phi'=0}[1,0]^T\Big\rangle, \tag{6}$$

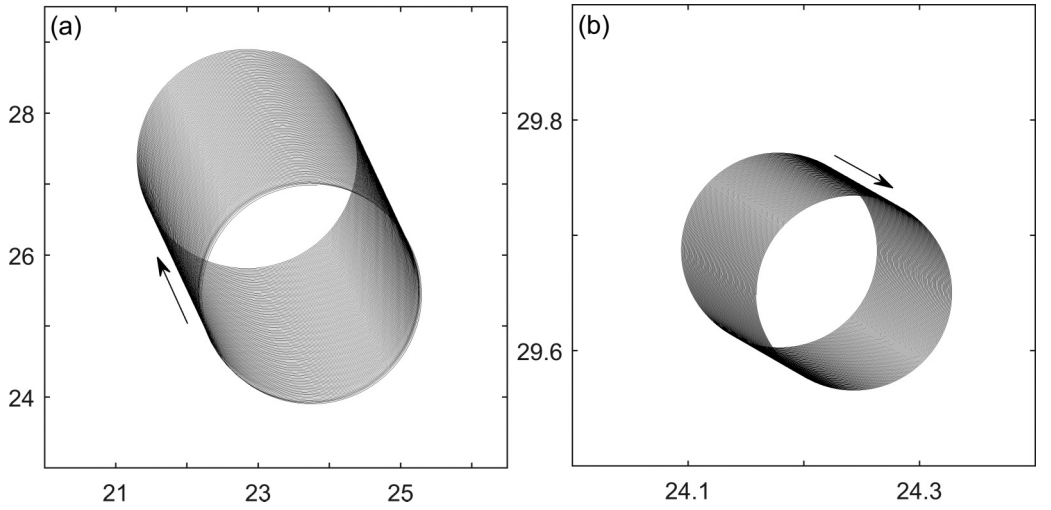

FIG. 5. Drift trajectories of spiral waves in the heterogeneous media with parameters $\varepsilon_0 = 0.02$ and $\delta = 0.0001$; (a) sparse spiral, and (b) dense spiral.

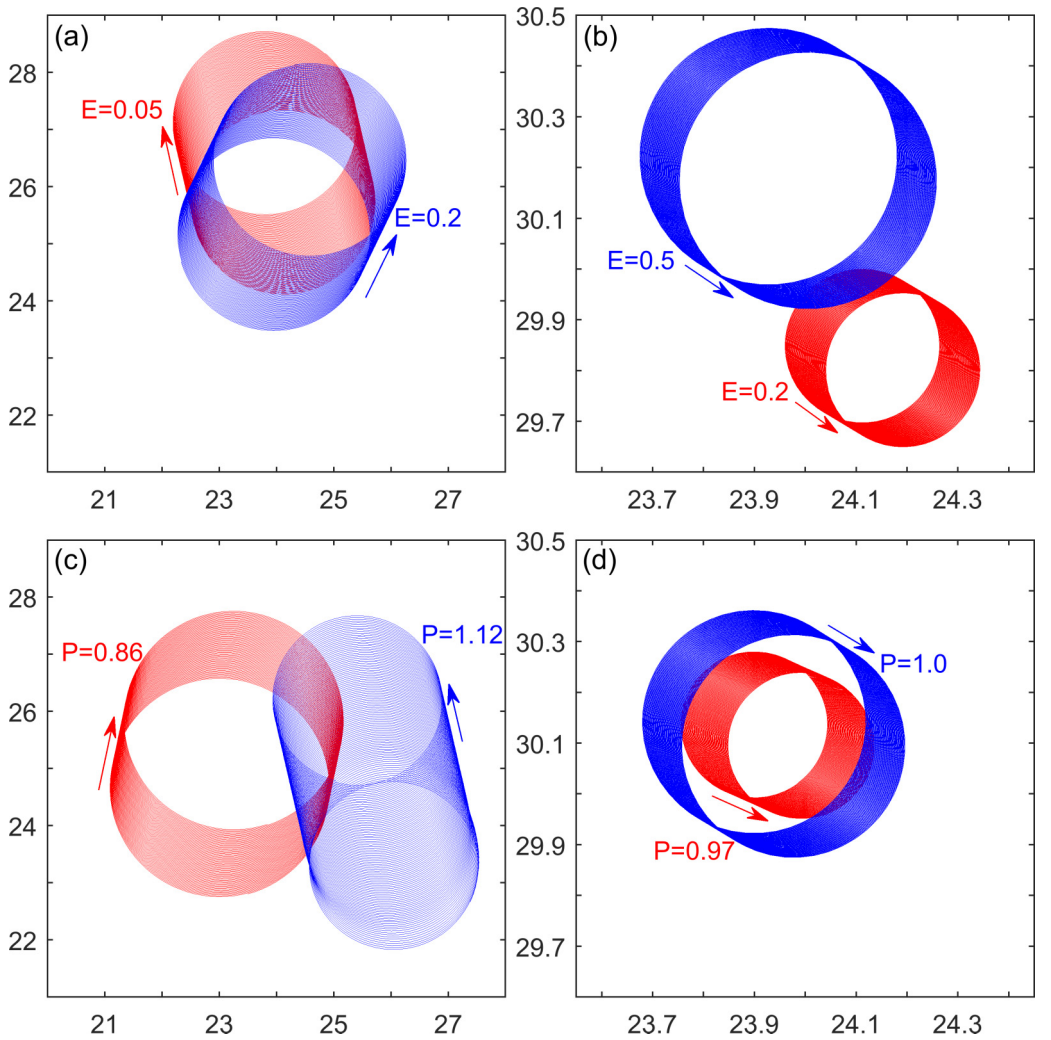

FIG. 6. Drift trajectories of synchronized spirals in the heterogeneous media with fixed parameters $\varepsilon_0 = 0.02$ and $\delta = 0.0001$. The parameters of external current are changed: (a) and (b) fixing the frequency rate $P = 1$ but changing the strength I_0, (c) and (d) fixing the strength $I_0 = 0.4$ but changing the frequency rate P. The left column corresponds to the sparse spirals, and the right corresponds to the dense.

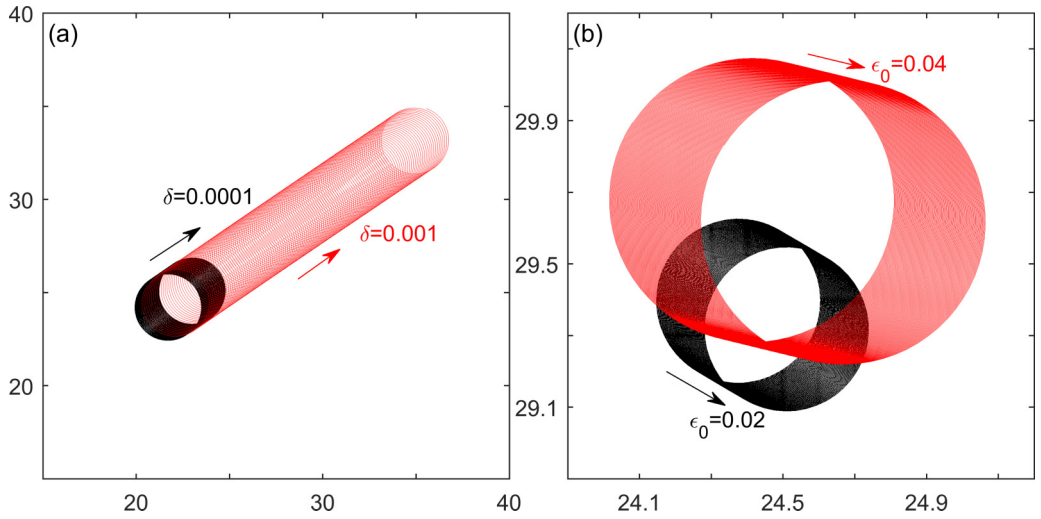

FIG. 7. (a) Drift trajectories of synchronized sparse spirals in the heterogeneous media with fixed $\varepsilon_0 = 0.02$ but changing δ. (b) Drift trajectories of synchronized dense spirals in the heterogeneous media with fixed $\delta = 0.0001$ but changing ε_0. The parameters of external current are fixed as $I_0 = 0.4$ and $P = 1$.

$$\dot{\Phi} = \varepsilon_0 \delta(x - x_0) \left\langle W^{(0)}(\rho, \theta, \Phi), \left[-\frac{1}{\varepsilon^2} U(1-U)\left(U - \frac{V+b}{a}\right)\right]|_{\Phi'=0}[1,0]^T \right\rangle. \tag{7}$$

The above equations show that spatial and temporal drifts are proportional to the heterogeneous parameter δ, and the temporal drift depends on x [46]. The numerical results in Fig. 5 verified the theoretical predictions. The theoretical values in the heterogeneous media of their drift speed and angle are $V = |\dot{R}| = 3.552 \times 10^{-3}$ and $\theta = 2.074$ for the sparse one, and $V = |\dot{R}| = 2.121 \times 10^{-4}$ and $\theta = -0.475$ for the dense one, respectively. The numerical values of their drift speed and angle are $V = |\dot{R}| = 3.440 \times 10^{-3}$ and $\theta = 2.011$ for the sparse one, and $V = |\dot{R}| = 2.113 \times 10^{-4}$ and $\theta = -0.531$ for the dense one, respectively. In all cases, numerical results show the quantitative agreement with the theoretical results. If one takes the external current into consideration, the derivations of Eqs. (6) and (7) are still applicable since the spiral is still in rigid rotation, only changing $\mathbf{W}$ to $\bar{\mathcal{W}}$ [40].

Moreover, the numerical drift speeds and angles of the sparse and dense spirals in the heterogeneous media by changing ε_0 and δ are shown in Fig. 8. The drift speed is linearly related to the change of δ, whether for sparse or dense spirals, which is also in good agreement with the relationship described by Eq. (6). But for ε_0, drift speed and ε_0 do not conform to the linear relationship. This is because the spiral wave is sensitive to the change of the parameter ε_0. With the shift of ε_0, the rigidly clockwise-rotating spiral wave solution $\mathbf{U}(\overrightarrow{r}, t)$ in Eq. (A3) also changes significantly; that is, the spiral wave has a large deformation. Therefore, the relationship between speed and parameter ε_0 is no longer linear. Furthermore, for both dense and sparse spirals, drift angles are determined by both Eqs. (6) and (7). Thus they correspond to the nonlinear relationship between ε_0 and δ.

V. CONCLUSION

In conclusion, we study drift dynamics of the sparse and dense spirals synchronized by suitable external current under another weak current or heterogeneity (or heterogeneous media). It should be noted that the joint external forces used in our methods can probably be stimulated in other disciplines, such as optogenetics [14,15] and sonogenetics [47,48], thus in many ways, our methods of controlling spiral wave drift can probably be clinically used [38]. However, previous methods concerning spiral wave drift mainly focused on chemical systems such as BZ reactions [13,18,19,21,36]. We can draw the following conclusions. First, the sparse spirals are much more easily synchronized by the external current than the dense ones. Moreover, synchronized sparse and dense spirals both execute directional drift induced by the weak current or heterogeneity, which is similar to that in [12]. Second, for sparse spiral waves, the media with negative filament tension can turn to positive under the influence of the external current, thus, if one extends the system to three dimensions, it would not break up into turbulence [41]. Similarly, the anomalous drift of the sparse spirals in the heterogeneous media can be changed easily to normal drift after synchronization, so that wave breaks in regions with longer spiral rotation period can be prevented. Thus our joint external forces are effective against "mother rotor" fibrillation, and can work as alternative low-energy technology to control electric turbulence. The proposed two-step procedure makes the spiral wave drift behaviors richer, and the scientists have more ways to manipulate the drift of the spiral waves. We hope that our findings can be observed in cardiac experiments.

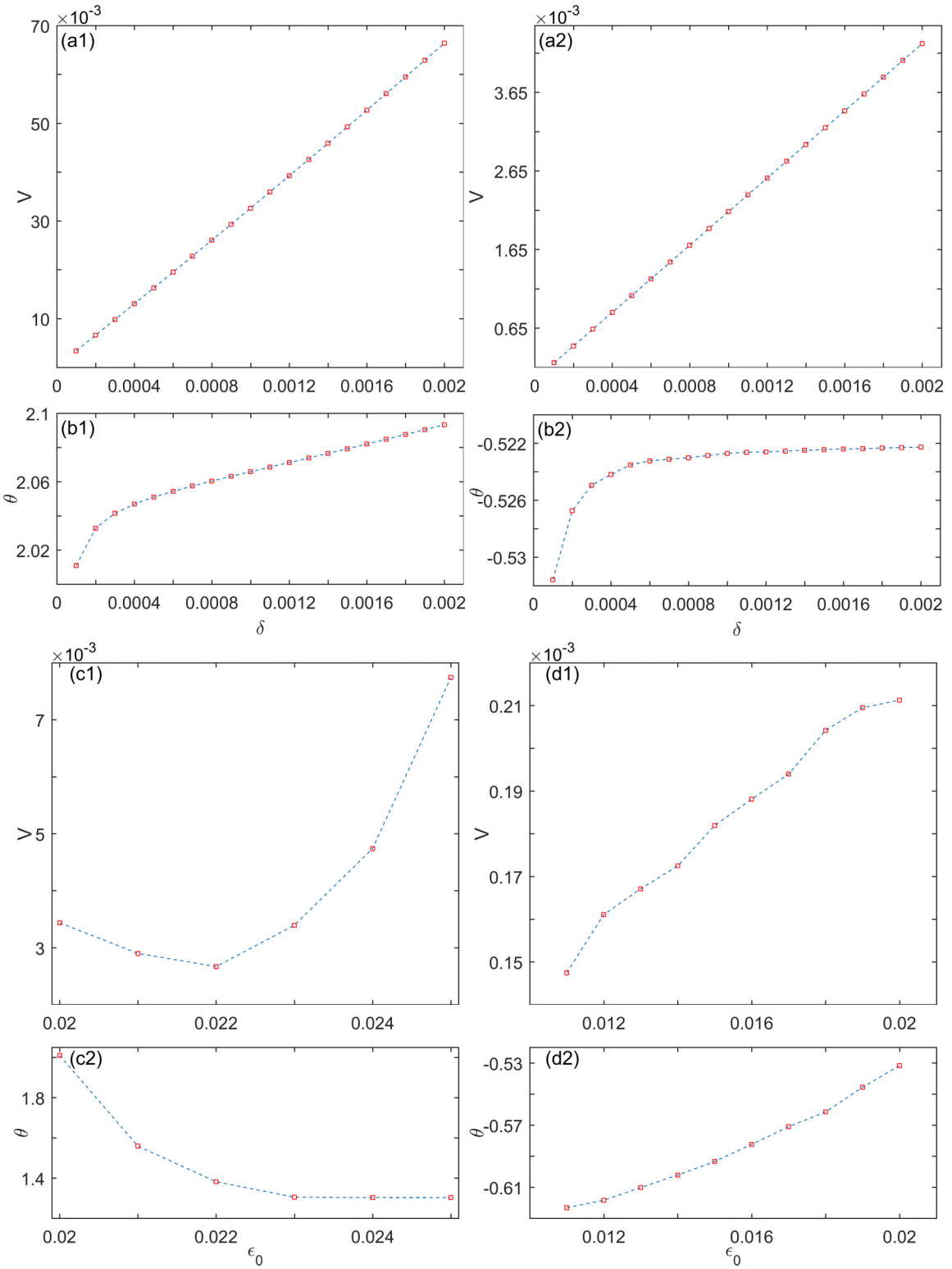

FIG. 8. Drift speeds and angles of the sparse and dense spirals in the heterogeneous media. (a),(b) Fixing $\varepsilon_0 = 0.02$ but changing δ. (c),(d) Fixing $\delta = 0.0001$ but changing ε_0. The left column corresponds to the sparse spiral, and the right corresponds to the dense spiral.

ACKNOWLEDGMENTS

This work was supported by the National Natural Science Foundation of China under Grants No. 12005066 and No. 12205059, Start-Up Funding of Hangzhou Normal University under Grant No. 4245C50223204004, and Natural Science Foundation of Guangxi Province in China under Grant No. 2018GXNSFBA050035.

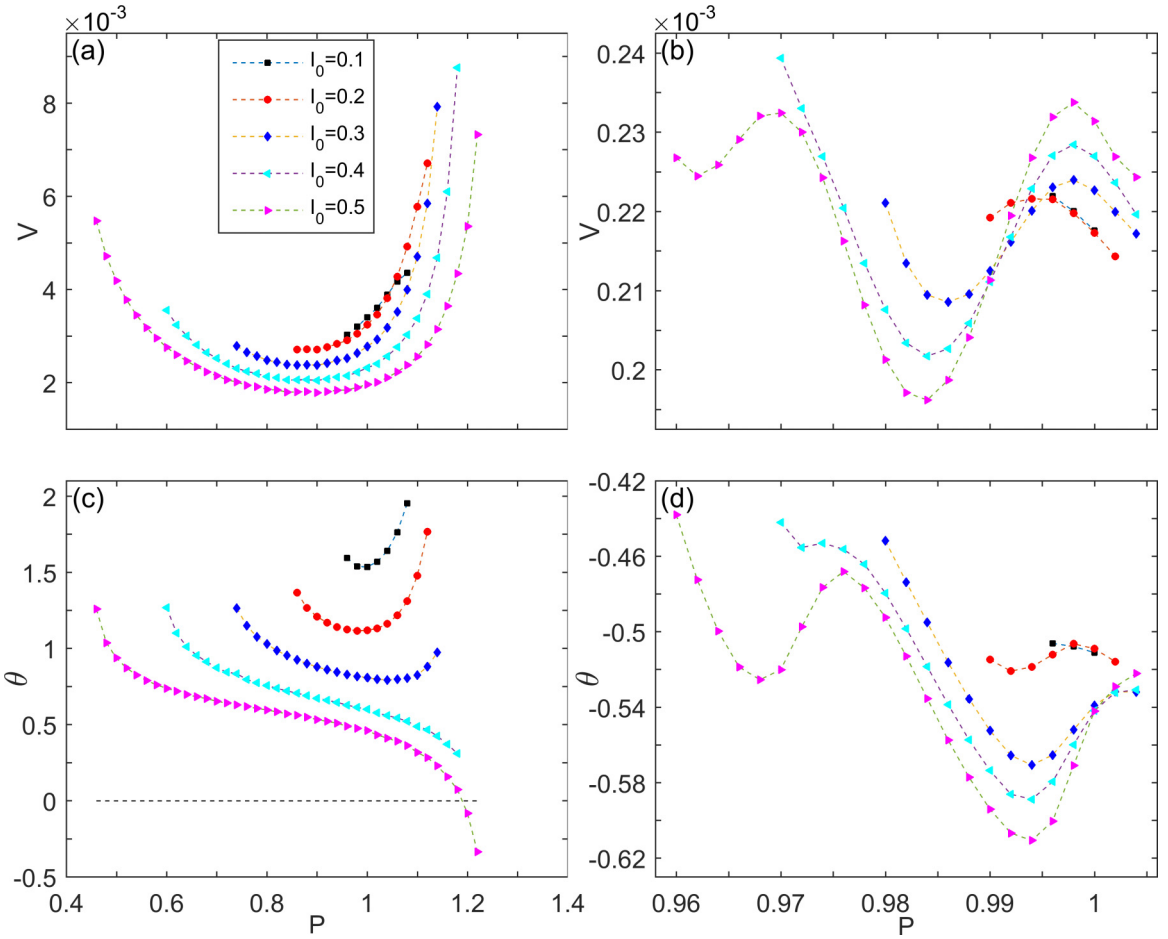

FIG. 9. Drift speeds and angles of the synchronized sparse and dense spirals in the heterogeneous media. The heterogeneous parameters are fixed as $\varepsilon_0 = 0.02$ and $\delta = 0.0001$, and the parameters of external current are changed. Panels (a) and (c) show drift speeds and angles of the sparse spirals; panels (b) and (d) correspond to the dense.

APPENDIX: RESPONSE FUNCTION THEORY FOR SPIRAL DRIFT IN HETEROGENEOUS MEDIA

To theoretically analyze the drift behavior of spiral waves in heterogeneous cardiac tissue, we rewrite the Barkley model in matrix form:

$$\partial_t \mathbf{u} = \mathbf{F}(\mathbf{u}, \varepsilon) + \widehat{\mathbf{D}\vec{\nabla}}^2 \mathbf{u}, \quad \varepsilon = \varepsilon_0[1 + \delta(x - x_0)], \quad \text{(A1)}$$

where $\mathbf{u} = [u, v]^T$, $\mathbf{F}(\mathbf{u}, \varepsilon) = [\varepsilon^{-1}u(1-u)[u-(v+b)/a], u-v]^T$, $\mathbf{D} = \mathrm{diag}(1, 0)$. The parameter ε has a small linear heterogeneities gradient in the parallel direction. If only the first order of Eq. (A1) is considered, the equation turns to

$$\partial_t \mathbf{u} = \mathbf{F}(\mathbf{u}, \varepsilon_0) + \widehat{\mathbf{D}\vec{\nabla}}^2 \mathbf{u} + \varepsilon_0\delta(x - x_0)\partial_\varepsilon \mathbf{F}(\mathrm{u}, \varepsilon_0)[1, 0]^T. \quad \text{(A2)}$$

$h(\mathbf{u}, \vec{r}, t) = \varepsilon_0\delta(x - x_0)\partial_\varepsilon \mathbf{F}(\mathrm{u}, \varepsilon_0)[1, 0]^T$ is the perturbation in the Cartesian coordinate system. For convenient calculation, x_0 is the center of the computation grids in the x axis and close to the rotation center of rigidly rotating spiral wave. In the absence of any heterogeneities, a rigidly clockwise-rotating spiral wave solution to Eq. (A2) has a convenient corotating polar coordinates form to analyze the drift velocity of the spiral:

$$\mathbf{U}(\overrightarrow{r}, t) = \begin{pmatrix} U(\rho(\overrightarrow{r} - \overrightarrow{R}), \vartheta(\overrightarrow{r} - \overrightarrow{R}) + \omega_e t - \Phi) \\ V(\rho(\overrightarrow{r} - \overrightarrow{R}), \vartheta(\overrightarrow{r} - \overrightarrow{R}) + \omega_e t - \Phi) \end{pmatrix}, \quad \text{(A3)}$$

where $\vec{R} = (x_0, y_0)^T$ is the rotation center of spiral wave, Φ is the spiral wave's initial rotation phase, $\omega_e > 0$ is the angular frequency of spiral wave, and $\rho(\overrightarrow{r} - \overrightarrow{R})$ and $\vartheta(\overrightarrow{r} - \overrightarrow{R})$ construct polar coordinates at rotation center $\overrightarrow{R}$. The spiral tip is $\overrightarrow{\zeta}_{tip}(t)$ rotating around rotation center $\overrightarrow{R}$. We choose the angle between $\vec{\zeta}_{tip}(t = 0) - \vec{R}$ and the x axis as the initial rotation phase Φ, which is measured counterclockwise from the positive x axis. In these corotating polar coordinates, the small perturbation turns to $h(\mathbf{u}, \vec{r}, t) = \delta\varepsilon_0[X - x_0 + \rho\cos(\vartheta)]\partial_\varepsilon \mathbf{F}(\mathbf{U}, \varepsilon_0)[1, 0]^T$, the polar angle is given by $\theta = \vartheta + \omega_e t - \Phi$, with $\overrightarrow{R'} = \vec{0}$ and $\Phi' = 0$ in the Cartesian coordinate system.

According to response function theory [46,49,50], the small perturbation $h(\mathbf{u}, \vec{r}, t)$ causing translational and rotational shifts of a spiral acts on the rigidly rotating spirals, and

we can obtain the drift velocity of spiral waves:

$$\dot{R}(t) = \varepsilon_0 \delta e^{i\Phi} \int_{t-\pi/\omega}^{t+\pi/\omega} \frac{\omega \mathrm{d}\tau}{2\pi} e^{-i\omega\tau} \langle \mathbf{W}^{(1)}(\rho, \theta, \Phi), [X - x_0 + \rho\cos(\vartheta)] \partial_\varepsilon \mathbf{F}(\mathbf{U}, \varepsilon_0)|_{\Phi'=0} [1, 0]^T \rangle, \tag{A4}$$

where $R(t) = X + iY$ is the complex coordinate of the instant spiral center, and $\dot{R}(t)$ is the drift velocity. The inner product $\langle \mathbf{w}, \mathbf{v} \rangle$ represents for the scalar product in the functional space in the spiral reference system ($\Phi' = 0$),

$$\langle \mathbf{w}, \mathbf{v} \rangle = \int \mathbf{w}^+(\rho, \theta) \mathbf{v}(\rho, \theta) \rho d\rho d\theta,$$

and $\mathbf{W}^{(1)}$ is one of the response functions of the spiral, that is, the eigenfunction of the adjoint linearized operator corresponding to the critical eigenvalue $-i\omega$.

After integration over the spiral wave rotation period, the drift velocity can be expressed as

$$\dot{R} = \varepsilon_0 \delta \left\langle \mathbf{W}^{(1)}(\rho, \theta, \Phi), \rho \frac{e^{-i\theta}}{2} \partial_\varepsilon \mathbf{F}(\mathbf{U}, \varepsilon_0)|_{\Phi'=0} [1, 0]^T \right\rangle. \tag{A5}$$

$\dot{R}$ can also be written as $\dot{R} = |\dot{R}| e^{i\Theta}$, where $|\dot{R}|$ is the drift speed and Θ is the drift direction.

Furthermore, we also can calculate the rotational frequency change of spiral wave:

$$\dot{\Phi} = \varepsilon_0 \delta \int_{t-\pi/\omega}^{t+\pi/\omega} \frac{\omega \mathrm{d}\tau}{2\pi} \langle \mathbf{W}^{(0)}(\rho, \theta, \Phi), [X - x_0 + \rho\cos(\vartheta)] \times \partial_\varepsilon \mathbf{F}(\mathbf{U}, \varepsilon_0)|_{\Phi'=0} [1, 0]^T \rangle. \tag{A6}$$

$\mathbf{W}^{(0)}$ is one of the response functions of the spiral wave with critical eigenvalue 0. After integration, one can get

$$\dot{\Phi} = \varepsilon_0 \delta (X - x_0) \langle \mathbf{W}^{(0)}(\rho, \theta, \Phi), \partial_\varepsilon \mathbf{F}(\mathbf{U}, \varepsilon_0)|_{\Phi'=0} [1, 0]^T \rangle. \tag{A7}$$

Substituting $\mathbf{F}(\mathbf{U})$ of the Barkley model into Eqs. (A5) and (A7), we obtain

$$\dot{R} = \varepsilon_0 \delta \left\langle W^{(1)}(\rho, \theta, \Phi), \rho \frac{e^{-i\theta}}{2} \left[-\frac{1}{\varepsilon^2} U(1 - U) \times \left(U - \frac{V + b}{a} \right) \right]|_{\Phi'=0} [1, 0]^T \right\rangle, \tag{A8}$$

$$\dot{\Phi} = \varepsilon_0 \delta (x - x_0) \left\langle W^{(0)}(\rho, \theta, \Phi), \left[-\frac{1}{\varepsilon^2} U(1 - U) \left(U - \frac{V + b}{a} \right) \right]|_{\Phi'=0} [1, 0]^T \right\rangle. \tag{A9}$$

We use the open-source software DXSPIRAL to calculate Eqs. (A8) and (A9) and thereby analyze the drift behavior of the spiral wave in heterogeneity.

[1] A. T. Winfree, Science **175**, 634 (1972).
[2] S. Jakubith, H. H. Rotermund, W. Engel, A. von Oertzen, and G. Ertl, Phys. Rev. Lett. **65**, 3013 (1990).
[3] N. A. Gorelova and J. Bures, J. Neurobiol. **14**, 353 (1983).
[4] S. Sawai, P. A. Thomason, and E. C. Cox, Nature (London) **433**, 323 (2005).
[5] R. A. Gray, A. M. Pertsov, and J. Jalife, Nature (London) **392**, 75 (1998).
[6] D. P. Zipes and J. Jalife, *Cardiac Electrophysiology: From Cell to Bedside* (Saunders, Philadelphia, 2004).
[7] S. V. Pandit and J. Jalife, Circ. Res. **112**, 849 (2013).
[8] S. Nattel, F. Xiong, and M. Aguilar, Nat. Rev. Cardiol. **14**, 509 (2017).
[9] R. W. Koster, P. Dorian, F. W. Chapman, P. W. Schmitt, S. G. O'Grady, and R. G. Walker, Am. Heart J. **147**, e1 (2004).
[10] C. F. Babbs, W. A. Tacker, J. F. VanVleet, J. D. Bourland, and L. A. Geddes, Am. Heart J. **99**, 734 (1980).
[11] M. Santini, C. Pandozi, G. Altamura, G. Gentilucci, M. Villani, M. C. Scianaro, A. Castro, F. Ammirati, and B. Magris, J. Interventional Card. Electrophysiol. **3**, 45 (1999).
[12] G. P. Walcott, C. R. Killingsworth, and R. E. Ideker, Resuscitation **59**, 59 (2003).
[13] K. I. Agladze, V. A. Davydov, and A. S. Mikhailov, JETP Lett. **45**, 767 (1987).
[14] R. A. B. Burton, A. Klimas, C. M. Amborsi, J. Tomek, and A. Corbett, Nat. Photonics. **9**, 813 (2015).
[15] T. C. Li, W. Zhong, B. Q. Ai, A. V. Panfilov, and H. Dierckx, Phys. Rev. E **105**, 014214 (2022).
[16] L. Xu, Z. Qu, and Z. Di, Phys. Rev. E **79**, 036212 (2009).
[17] S. Sridhar, S. Sinha, and A. V. Panfilov, Phys. Rev. E **82**, 051908 (2010).
[18] T. C. Li, X. Gao, F. F. Zheng, D. B. Pan, B. Zheng, and H. Zhang, Sci. Rep. **7**, 8657 (2017).
[19] O. Steinbock, J. Schütze, and S. C. Müller, Phys. Rev. Lett. **68**, 248 (1992).
[20] J. Lee, J. Kim, G. H. Yi, and K. J. Lee, Phys. Rev. E **65**, 046207 (2002).
[21] V. Krinsky, E. Hamm, and V. Voignier, Phys. Rev. Lett. **76**, 3854 (1996).
[22] O. Steinbock, V. Zykov, and S. C. Müller, Nature (London) **366**, 322 (1993).
[23] V. Zykov, O. Steinbock, and S. C. Müller, Chaos **4**, 509 (1994).
[24] M. Braune, A. Schrader, and H. Engel, Chem. Phys. Lett. **222**, 358 (1994).
[25] A. Schrader, M. Braune, and H. Engel, Phys. Rev. E **52**, 98 (1995).
[26] S. Nettesheim, A. von Oertzen, H. H. Rotermund, and G. Ertl, J. Chem. Phys. **98**, 9977 (1993).
[27] V. S. Zykov, G. Bordiougov, H. Brandtstädter, I. Gerdes, and H. Engel, Phys. Rev. E **68**, 016214 (2003).
[28] H. Zhang, N. J. Wu, H. P. Ying, G. Hu, and B. Hu, J. Chem. Phys. **121**, 7276 (2004).
[29] S. Kantrasiri, P. Jirakanjana, and O. -U. Kheowan, Chem. Phys. Lett. **416**, 364 (2005).
[30] L. Xu, Z. Li, Z. Qu, and Z. Di, Phys. Rev. E **85**, 046216 (2012).
[31] A. Mikhailov, V. Davydov, and V. Zykov, Phys. D (Amsterdam, Neth.) **70**, 1 (1994).
[32] R. M. Mantel and D. Barkley, Phys. Rev. E **54**, 4791 (1996).

[33] V. Hakim and A. Karma, Phys. Rev. E **60**, 5073 (1999).
[34] J. Langham and D. Barkley, Chaos **23**, 013134 (2013).
[35] J. Langham, I. Biktasheva, and D. Barkley, Phys. Rev. E **90**, 062902 (2014).
[36] J. Luo, T. C. Li, and H. Zhang, Phys. Rev. E **101**, 032205 (2020).
[37] S. Luther, F. H. Fenton, B. G. Kornreich, A. Squires, P. Bittihn, D. Hornung, M. Zabel, J. Flanders, A. Gladuli, L. Campoy, E. M. Cherry, G. Luther, G. Hasenfuss, V. I. Krinsky, A. Pumir, R. F. Gilmour Jr., and E. Bodenschatz, Nature (London) **475**, 235 (2011).
[38] A. V. Panfilov, Phys. Rev. Lett. **88**, 118101 (2002).
[39] D. Barkley, Phys. D (Amsterdam, Neth.) **49**, 61 (1991).
[40] T. C. Li, B. W. Li, B. Zheng, H. Zhang, A. Panfilov, and H. Dierckx, New J. Phys. **21**, 043012 (2019).
[41] T. C. Li, X. Gao, F. F. Zheng, M. C. Cai, B. W. Li, H. Zhang, and H. Dierckx, Phys. Rev. E **93**, 012216 (2016).
[42] S. Alonso and A. V. Panfilov, Phys. Rev. Lett. **100**, 218101 (2008).
[43] S. Alonso, M. Bär, and A. V. Panfilov, Bull. Math. Biol. **75**, 1351 (2013).
[44] V. N. Biktashev, A. V. Holden, and H. Zhang, Philos. Trans. R. Soc. London Ser. A **347**, 611 (1994).
[45] H. Henry and V. Hakim, Phys. Rev. E **65**, 046235 (2002).
[46] I. V. Biktasheva, D. Barkley, V. N. Biktashev, and A. J. Foulkes, Phys. Rev. E **81**, 066202 (2010).
[47] S. Ibsen, A. Tong, C. Schutt, S. Esener, and S. H. Chalasani, Nat. Commun. **6**, 1 (2015).
[48] M. D. Menz, P. Ye, K. Firouzi, A. Nikoozadeh, K. B. Pauly, P. Khuri-Yakub, and S. A. Baccus, J. Neurosci. **39**, 6251 (2019).
[49] V. Biktashev and A. Holden, Chaos Solitons Fractals **5**, 575 (1995).
[50] I. V. Biktasheva, D. Barkley, V. N. Biktashev, G. V. Bordyugov, and A. J. Foulkes, Phys. Rev. E **79**, 056702 (2009).